Evolution of Classical 1-D-Based Models and Improved Approach for the Characterization of Litz Wire Losses

Asier Arruti, Iosu Aizpuru, Mikel Mazuela, Ziwei Ouyang, and Michael A.E. Andersen

***Abstract*—Prediction of Litz wire losses is a challenging endeavor in the design of high-frequency transformers. Although many analytical approaches of varying complexity can be found in the literature, classical 1-D-based models are the norm in the analysis of wide design spaces. Even then, an important degree of uncertainty exists around the accuracy of the 1-D models. After a critical review of these models and an analysis of their application in Litz wire loss prediction, a new model is proposed, which tries to address some of the concerns and limitations of the existing approaches. The models are evaluated against 2-D finite-element simulations in many different conditions to ensure that the models correctly consider the impact of different parameters. The experimental results are presented to demonstrate the accuracy of the new approach at very high frequencies and high amounts of strands using four prototypes with different Litz wires, designed to correctly match the conditions inherent to any 1-D model.**

***Index Terms*—Copper losses, high-frequency transformer, Litz wire, mathematical models.**

I. Introduction

In THE design of power electronics' converters, the accurate representation of component behavior is critical for the optimal design of the converter. The magnetic devices (transformers and inductors) play a major role in the overall efficiency, power density, weight, and cost of the design [1], [2], [3], [4], and should be accordingly designed for each specific application.

The inclusion of wide band gap technologies (GaN and SiC transistors) allows to increase the power converter switching frequencies beyond the typical limits of silicon-based inuslated gate bipolar transistor (IGBT) and MOSFET switches [5], [6]. It is well known that the increase in frequency can aid in the reduction of magnetic device size, but this scaling law is limited by the power loss and dissipation capabilities of the devices [1], [2], [3], [4], [7]. For transformer design, the optimal design frequency of the transformer can range between 10 and 20 kHz for applications in the range of hundreds of kilowatts [8], [9], [10], to beyond the megahertz range for applications up to the kilowatt limit [11], [12], [13], [14].

One of the functional constraints in these high-frequency transformers is the winding temperature, which becomes complex to evaluate due to the nature of high-frequency copper losses. These high-frequency losses are primarily due to skin and proximity effects, although in specific cases, such as hybrid/integrated magnetics, the fringing effect can also be a major contributor [15], [16], [17], [18]. Litz wire, comprised of transposed insulated strands, can effectively decrease the skin and proximity effects associated with high frequencies, but despite its efficacy in reducing these losses, the accurate modeling of Litz wire losses is a challenging endeavor.

A priori, the accurate estimation of Litz wire losses might not appear critical in the examples shown above; lower power applications planar magnetics with printed circuit board (PCB) windings are used in many cases [11], [12], [13], [14], but design utilizing Litz wire may still offer significant advantages [6], [19], [20], [21], or even hybrid PCB-Litz windings might be used [22], [23]. For higher power applications, although the frequencies are much lower than their planar counterparts [8], [9], [10], due to the requirement of much higher copper cross sections, which usually entails higher amounts of strands, the selection of Litz wire has a nonmarginal impact in the transformer cost, as shown by the cost trends from [24] and [25].

Finite-element simulations of the intricate internal geometry are in most cases too computationally heavy for the design process of the transformer; thus, analytical approaches are generally preferred. Even though complex analytical models can be found in the literature tackling this problem, classical 1-D-based approaches, namely Dowell's [26] and Ferreira's [27], [28] methods, are still the norm when it comes to the preliminary evaluation of wide transformer design spaces [4], [8], [10].

Even then, there is still a noticeable uncertainty level around which of these approaches is the best to use, and disagreeing conclusions can be found in the literature [27], [28], [29], [30], [31], [32]. Thus, this article tries to address these concerns while presenting the following main contributions.

1) Review of classical 1-D models analysis of the use of these models in the literature publications.

Received 12 February 2024; revised 29 June 2024; accepted 5 August 2024. Date of publication 21 August 2024; date of current version 7 October 2024. This work was supported by the Department of Education of the Basque Government under the Non-Doctoral Research Staff Training Program under Grant PRE_2020_1_0267. Recommended for publication by Associate Editor J. M. Alonso. *(Corresponding author. Asier Arruti.)*

Asier Arruti, Iosu Aizpuru, and Mikel Mazuela are with the Faculty of Engineering, Mondragon University, Mondragon 20500, Spain (e-mail: aarruti@mondragon.edu; iaizpuru@mondragon.edu; mmazuela@mondragon.edu).

Ziwei Ouyang and Michael A.E. Andersen are with the Department of Electrical and Photonics Engineering, Technical University of Denmark, Kgs. Lyngby, Denmark (e-mail: ziou@dtu.dk; maea@dtu.dk).

Color versions of one or more figures in this article are available at https://doi.org/10.1109/TPEL.2024.3446962.

Digital Object Identifier 10.1109/TPEL.2024.3446962

2) Proposal of two alternative models with modifications from Dowell's and Ferreira's models.
3) Development of a simulation methodology for fast 2-D finite element method (FEM) simulations for the high number of Litz strands, using a more realistic Litz wire internal strand distribution.
4) Experimental evaluation of Litz wires' losses in very high frequencies.

The rest of this article is organized as follows. Section II serves as a review of these classical 1-D models and their application to the problem of Litz wire losses, while Section III presents two alternative approaches to model these losses. Comparison of these models against various 2-D finite-element simulations of transformer winding configurations is shown in Section IV, where Litz wires of up to 1000 strands are evaluated, and the validation against experimental results from transformers adhering to the classical 1-D geometries is included in Section V. Finally, Section VI concludes this article.

II. Review of the Existing 1-D Models and Their Applications to Litz Wires

For the solution of high-frequency losses in copper windings for transformers, two approaches based on the exact mathematical solutions of Maxwell's electromagnetic equations can be found: Dowell's method [26] and Ferreira's method [27], [28]. Note that, although both approaches are commonly named after the respective article's authors, the mathematical solutions of these problems can be dated back to previous works: solutions for rectangular windings resembling those presented by Dowell can be found in 1940 [33], and solutions for cylindrical windings close to Ferreira's formulations are found in 1922 [34]. Still, for the sake of simplicity and familiarity, the approaches will be classified into models based on Dowell's approach (solution for rectangular wires) and models based on Ferreira's approach (solution for circular wires).

Both approaches use an equivalent high frequency resistance to define the power losses P_{loss} as a function of effective current

$$P_{\text{loss}} = I_{\text{rms}}^2 \cdot (R_{\text{DC}} \cdot F_R) \tag{1}$$

where the equivalent high frequency resistance is the dc resistance R_{DC} multiplied by the resistance ratio F_R.

A. Dowell's Approach

The Dowell's solution for F_R is obtained when Maxwell's electromagnetic equations are solved for an infinitely tall rectangular conductor under the assumption of unidimensional field (in the y-direction), as shown in Fig. 1(a). This situation is equivalent to finite rectangular conductors placed between two high permeability mediums, which is a common case in foil transformer windings. In these circumstances, according to Dowell's work [26], the average F_R value for the windings takes the form, although other equivalent forms can be found in [33] and [35]. Here, m is the number of layers (number of conductors in the x-direction) and Δ is the penetration depth defined as a function of the skin depth δ for a given frequency f, conductivity σ, and permeability μ. In the case of transformers, the winding area permeability (air) is used so that $\mu = 4\pi \cdot 10^{-7}$

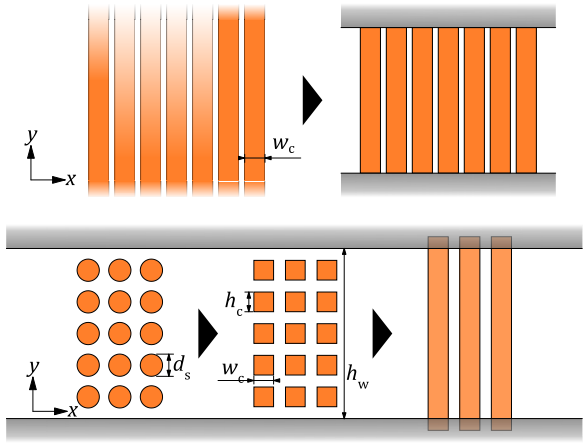

Fig. 1. (a) Winding structure for the Dowell approach and (b) application to cylindrical conductors.

$$F_R = \Delta\left(\frac{\sin h2\Delta + \sin 2\Delta}{\cos h2\Delta - \cos 2\Delta} + \frac{2\left(m^2-1\right)}{3}\frac{\sin h\Delta - \sin\Delta}{\cos h\Delta + \cos\Delta}\right) \tag{2}$$

$$\Delta = \frac{w_c}{\delta} \tag{3}$$

$$\delta = \sqrt{\pi f \sigma \mu}^{-1}. \tag{4}$$

The case presented in [26] assumes that the conductors occupy the full window area height, but this is rarely the case in real transformers since they are usually made of various conductors with gaps in the y-direction. The 1-D magnetic field in the borders of a layer of N vertically stacked conductors is equal to a solid layer carrying N times the current; thus, Dowell considers that the F_R of a layer of N vertically stacked rectangular conductors is the same as a solid layer of equivalent conductivity, as shown in Fig. 1(b). Then, the skin depth is modified so that

$$\delta' = \sqrt{\eta}^{-1}\,\delta \tag{5}$$

$$\eta = N\frac{h_c}{h_w} \tag{6}$$

where δ' is the "effective skin depth," and η is the ratio between the height occupied by the conductors $N \cdot h_c$ to the height of the winding area h_w, referred to as "conductor spacing factor," "layer porosity," "layer copper factor," or most commonly "porosity factor." In the case of cylindrical wires of diameter d, Dowell first transforms these into rectangular conductors of equal cross section so that the height and width of the conductors are given as follows and then solves the problem using the proper porosity factor:

$$h_c = w_c = \sqrt{\frac{\pi}{4}}\,d. \tag{7}$$

Note that the transformation from circular to square conductors using the same cross section is not supported by any physical meaning [27], [36], and the relation of $w_c = (3\pi/16)^{1/4}\ d$

has been found to give better results [37]. Also, several works have pointed out that the porosity factor entails an error in Dowell's calculations since skin depth as a physical parameter cannot be influenced by the porosity factor [27], and Ampere's law is mismatched for $\eta \neq 1$ [36]; thus, Dowell's approach is considered only accurate for high-porosity factors.

B. Ferreira's Approach

To evaluate high-frequency copper losses with circular conductors circumventing the intrinsic problems from Dowell's approach, Ferreira presented another method using the mathematical solution in cylindrical coordinates based on the Bessel functions [27], [28]. To do so, Ferreira's work uses the orthogonality principle between skin and proximity losses, postulated in [38], meaning that both loss phenomena can be calculated independently and added together. This can be demonstrated by Dowell's approach, where (2) can be rewritten as follows:

$$F_{R,m} = \frac{\Delta}{2}\left(\frac{\sin h\Delta + \sin\Delta}{\cos h\Delta - \cos\Delta} + (2m-1)^2 \frac{\sin h\Delta - \sin\Delta}{\cos h\Delta + \cos\Delta}\right) \tag{8}$$

where $F_{R,m}$ is defined per layer instead of the average F_R of the winding section. Here, the first term is equal to the solution of the skin effect for square conductors; thus, according to the orthogonality, the second term defines the proximity losses in the mth layer. As demonstrated by Perry [35], the term $(2m-1)$ relates to the magnetic field strength applied to each layer, so it can be concluded that the losses grow as a function of the square of this applied magnetic field.

In this case, the losses for circular conductors can be obtained by first solving the skin and proximity losses independently and adding them together. The resulting expression for circular wires is

$$F_{R,m} = \frac{\gamma}{2}\left(\frac{\mathrm{ber}\,\gamma\,\mathrm{bei}'\,\gamma - \mathrm{bei}\,\gamma\,\mathrm{ber}'\gamma}{\mathrm{ber}'^2\,\gamma + \mathrm{bei}'^2\,\gamma}\right.$$

$$\left. -2\pi(2m-1)^2 \frac{\mathrm{ber}_2\,\gamma\,\mathrm{ber}'\,\gamma + \mathrm{bei}_2\,\gamma\,\mathrm{bei}'\gamma}{\mathrm{ber}^2\,\gamma + \mathrm{bei}^2\,\gamma}\right) \tag{9}$$

where ber and bei are the Kelvin functions, representing the real and imaginary parts of the Bessel function, respectively, and in this case

$$\gamma = \frac{d}{\delta\sqrt{2}} \tag{10}$$

is the adapted definition for the penetration depth in round conductors.

The expression achieved in [27] is based on [26] with modified functions since Ferreira simply replaces the skin effect and proximity effect expressions with the ones for circular wires. This is purposely done to compare the discrepancies in the F_R values with Dowell's results. This does not mean that (9) can be used as is since Ferreira clearly expresses the limitations of the porosity factor proposed by Dowell. Based on Ferreira's demonstration, the more adequate definition for high-frequency square conductor losses taking the orthogonality principle is

$$F_{R,m} = S_R + G_R H_e^2 \tag{11}$$

$$S_R = \frac{\Delta}{2}\frac{\sin h\Delta + \sin\Delta}{\cos h\Delta - \cos\Delta} \tag{12}$$

$$G_R = \frac{\Delta}{2}\frac{\sin h\Delta - \sin\Delta}{\cos h\Delta + \cos\Delta} \tag{13}$$

where S_R and G_R are the skin and proximity factors, respectively, and H_e is the external magnetic field applied to the conductor. The analog factors for round conductors are then

$$S_R = \frac{\gamma}{2}\frac{\mathrm{ber}\,\gamma\,\mathrm{bei}'\,\gamma - \mathrm{bei}\,\gamma\,\mathrm{ber}'\gamma}{\mathrm{ber}'^2\,\gamma + \mathrm{bei}'^2\,\gamma} \tag{14}$$

$$G_R = -\gamma\pi\frac{\mathrm{ber}_2\,\gamma\,\mathrm{ber}'\,\gamma + \mathrm{bei}_2\,\gamma\,\mathrm{bei}'\gamma}{\mathrm{ber}^2\,\gamma + \mathrm{bei}^2\,\gamma}. \tag{15}$$

The porosity factor also relates the field generated by a solid conductor occupying the full winding area height and the magnetic field generated by conductors not occupying the full height, as illustrated in Fig. 1(b). Thus, taking this reduction of the magnetic field should result in a more accurate description of high-frequency losses for square conductors than (8), where Δ is calculated with δ instead of δ'. It follows that the same logic must be applied to (9) for cases where $\eta \neq 1$. Ferreira does not present such an equation and instead proposes to evaluate the magnetic field generated by the rest of the wires and use this in the calculations avoiding the necessity of η, resulting in a more generalized solution. An expression based in (9) with the inclusion of the porosity factor can be found in [39] and [40], taking the form but is limited to transformers with winding layers composed of the same number of round conductors

$$F_{R,m} = \frac{\Delta}{2}\left(\frac{\sin h\Delta + \sin\Delta}{\cos h\Delta - \cos\Delta}\right.$$

$$\left. + \eta^2(2m-1)^2\frac{\sin h\Delta - \sin\Delta}{\cos h\Delta + \cos\Delta}\right) \tag{16}$$

$$F_{R,m} = \frac{\gamma}{2}\left(\frac{\mathrm{ber}\,\gamma\,\mathrm{bei}'\,\gamma - \mathrm{bei}\,\gamma\,\mathrm{ber}'\gamma}{\mathrm{ber}'^2\,\gamma + \mathrm{bei}'^2\,\gamma}\right.$$

$$\left. -2\pi\eta^2(2m-1)^2\frac{\mathrm{ber}_2\,\gamma\,\mathrm{ber}'\,\gamma + \mathrm{bei}_2\,\gamma\,\mathrm{bei}'\gamma}{\mathrm{ber}^2\,\gamma + \mathrm{bei}^2\,\gamma}\right). \tag{17}$$

Remark that, in the Dowell's based approximation with conductors filling the complete vertical height, $(2m-1)$ term from (8) related to H_e is present even in single-layer windings. Using the 1-D field generated by all the wires in the evaluation of H_e instead of the rest of the wires results in a better mathematical implementation of the orthogonality principle for typical transformer configurations.

Although Ferreira's approach is based on the Bessel function solutions for circular wires, many authors have reported better accuracy using Dowell's approach combined with the equivalent cross-sectional transformation (7), [30], [32], [36]. Note that the comparison from [32] might not be the most reliable due to some flaws detected in the analysis.

1) The *Dowell method (Dowell 1)* and *modified Dowell method (Dowell 2)* models, equivalent to (2), are presented as different models when the first is a specific case from the second.

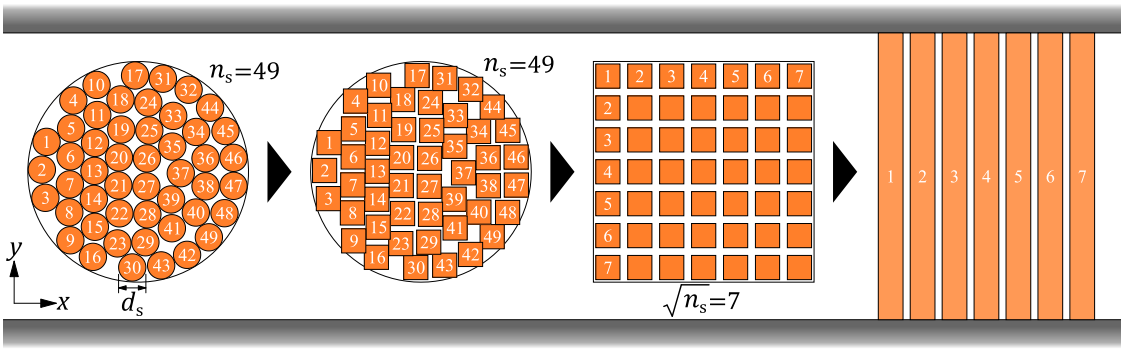

Fig. 2. Transformation of Litz wire of n_s circular strands into rectangular strands and rearranged into an $\sqrt{n_s}$ by $\sqrt{n_s}$ matrix to apply Dowell's approach.

2) The *Ferreira method (Ferreira 1)* model, analog to (14), not only applies the porosity factor to reduce the external field but also uses δ', thus overcorrecting the losses due to the proximity effect.
3) The *original Ferreira method (Ferreira 2)* and *modified Ferreira method (Reatti)* models, equivalent to (9) and (15), are presented as different models when the first is a specific case from the second as demonstrated above.
4) The ratio between the *original Ferreira method (Ferreira 2)* and *modified Ferreira method (Reatti)* model power losses, (9) and (15), cannot differ by a factor lower than η^2 (assuming 100% proximity losses), while the reported results appear to go beyond this limit. Note that the format of the presented results (3-D contour maps) complicates the extraction of precise data to prove this point.
5) The results displayed differ noticeably from those reported in [30], where typical errors of ∼5% and ∼1% are presented for Dowell's and Ferreira's models, respectively, in the low-frequency regions.

C. Litz Loss Modeling With 1-D Approaches

The application of the 1-D approaches to Litz wire conductors encompasses new challenges for the geometrical definition of the problems. To do so, two approaches can be identified in the literature: the transformation of the Litz wire into equivalent winding layers and the addition of the internal proximity factor to the losses.

1) Dowell's Equation on Litz Wires (Wojda's Approach): The concept behind the first approach is illustrated in Fig. 2, where each Litz wire bundle composed of n_s number of strands is transformed into a square wire matrix of $\sqrt{n_s}$ by $\sqrt{n_s}$ strands [41]. Then, it follows that the porosity factor (6) is modified as

$$\eta = N\sqrt{n_s}\sqrt{\frac{\pi}{4}}d_s/h_w \tag{18}$$

where $\sqrt{\pi/4}d_s$ is the equivalent square strand width of each circular strand using the cross-sectional transformation (7).

Then, the problem can be solved using (8) where

$$\Delta = \sqrt{\frac{\pi}{4}}d_s/\delta\sqrt{n} \tag{19}$$

is the penetration ratio according to Dowell [26] or using (15) where

$$\Delta = \sqrt{\frac{\pi}{4}}d_s/\delta \tag{20}$$

is the penetration ratio for the external magnetic field correction method proposed in [27].

Geometrical transformation also means that the number of winding layers has increased by a factor $\sqrt{n_s}$. Since the definition of layer loses physical meaning in this case, instead of obtaining the equivalent $F_{R,m}$ for a specific layer, the average F_R of all winding layers must be used to solve the problem. Transforming (8) and (15) back into an analog form of (2) results in and using Ferreira's modified Dowell's equation with unmodified skin effect

$$F_R = \frac{\Delta}{2}\left(\frac{\sin h\Delta + \sin\Delta}{\cos h\Delta - \cos\Delta} + \left(\frac{4\left(n_s\cdot m^2-1\right)}{3}+1\right)\frac{\sin h\Delta - \sin\Delta}{\cos h\Delta + \cos\Delta}\right) \tag{21}$$

$$F_R = \frac{\Delta}{2}\left(\frac{\sin h\Delta + \sin\Delta}{\cos h\Delta - \cos\Delta} + \eta^2\frac{2\left(n_s\cdot m^2-1\right)}{3}\frac{\sin h\Delta - \sin\Delta}{\cos h\Delta + \cos\Delta}\right). \tag{22}$$

This approach was popularized by Wojda and Kazimierczuk [31], and thus is commonly referred to as Wojda's approach, although as explained before, the concept of transformation of Litz strands into a square grid was presented previously by Van den Bossche and Valchev [[41], eq. (2.23)]

$$F_R = \Delta\cdot\left(\frac{\sin h2\Delta + \sin 2\Delta}{\cos h2\Delta - \cos 2\Delta} + 0.95\frac{2\left(n_s\cdot m^2-1\right)}{3}\frac{\sin h\Delta - \sin\Delta}{\cos h\Delta + \cos\Delta}\right). \tag{23}$$

Here, some minor modifications and correction factors are added to improve the accuracy of the results based on the following.

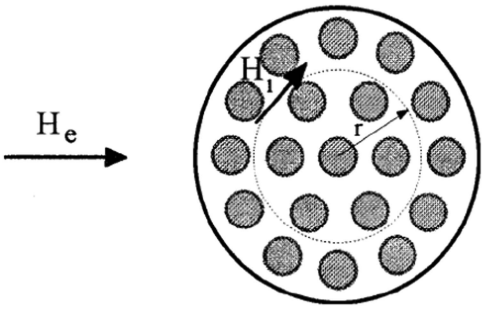

Fig. 3. External magnetic field H_e generated by the rest of the wires and the internal magnetic field H_i generated by the strands [39].

1) The formulations for the penetration depth and porosity factor are defined as

$$\Delta = \left(\frac{\pi}{4}\right)^{3/4} \frac{d_s}{\delta}\sqrt{n} \tag{24}$$

$$\eta = \sqrt{n_s}\, N \frac{d_s}{h_w} \tag{25}$$

where instead of using the strategy originally described by Dowell [26], the porosity factor is defined using the diameter of the circular conductor. Mathematically, both approaches are equivalent, but the definition (6) loses physical sense.

1) The proximity effect losses are decreased by a factor of 0.95 (π/3) according to the findings reported by Van den Bossche and Valchev [41]. Unlike in expression (8), the proximity losses in expression (2) are not solely represented by the second term (the first term combines eddy losses and a part of the proximity losses as demonstrated by Ferreira [27]); thus, a small error is introduced in the implementation of this correction factor. Still, the error introduced is negligible in most practical cases with Litz wires.

2) Ferreira's Approach for Litz Wires: Ferreira [42] proposes another approach to model Litz wire high-frequency losses. Instead of reordering the Litz wire strands into a matrix, the external magnetic field applied to the Litz wire (average H_e value, or H_e value in the center of the Litz wire bundle) and the internal collective field of the stranded conductors (H_i) are used, as illustrated in Fig. 3.

The Litz strand power losses due to the internal magnetic field are as follows:

$$P_i = \frac{G_R I_b^2}{8\pi^2 r_b^2 n_s} \tag{26}$$

where I_b is the total current in the Litz bundle and r_b is the radius of the Litz bundle [42]. Then, from the demonstration of orthogonality between H_e and H_i, it follows that the high-frequency losses are

$$F_{R,m} = S_R\, I^2 + G_R \left(H_e^2 + H_i^2\right) \tag{27}$$

and H_i is derived from (22)

$$H_i = \frac{I_b}{\sqrt{2}\cdot 2\pi \cdot r_b \sqrt{n_s}} \tag{28}$$

It follows that the γ parameter is defined using the Litz wire strand diameter, not the Litz wire bundle diameter.

A similar approach is presented in [39], where the losses due to the external magnetic field H_e and internal magnetic field H_i are taken separately, but the power loss definitions are normalized as functions of layer m instead of magnetic fields (porosity factors mathematically defined). Unfortunately, the approach from [39] has some caveats compared with [42].

1) The skin effect factor S_R is divided by the number of strands; thus, at very low frequencies, where $\gamma \ll d_s$ and proximity losses are negligible ($G_R \approx 0$), F_R becomes $1/n_s$.
2) The internal Litz field losses are multiplied by the layer term, meaning that these increase as a function of the number of layers. This goes against the orthogonality principle between external and internal Litz wire losses described in [42].
3) The definition of an external porosity factor η_1 for the external field and an internal porosity factor η_2 for the internal field is mentioned, which makes physical sense, but only η_1 can be described, as the Litz wire strands are distributed in 2-D and η describes a 1-D distribution. According to Bartoli et al. [39], turn-to-turn, layer-to-layer, and strand-to-strand distances are to consider when defining η_2, as well as the nonuniformity of the magnetic field, but no further explanations of how to do so are given.

Despite the different attempts to implement these equations, the approach from [39] did not yield satisfactory results, with error orders of magnitudes higher than the rest of the models tested in Section III.

III. Proposed Models

In Ferreira's approach for Litz wire models, two sources of proximity losses are assumed, proximity losses generated by the external magnetic field H_e and proximity losses from the internal collective magnetic field H_i. The problem with this assumption is that it does not accurately depict the classical transformer geometry where the 1-D field analysis is valid. When the Litz wire is structured in layers inside the core window, the 1-D magnetic field across the x-dimension is not constant, taking the form of a sigmoid due to the circular geometry of the Litz wire. Since the proximity losses grow quadratically with H_e, this average field results in an underestimation of the losses.

For the transformer winding structure in interest, alternatively, the classical 1-D field assumption can be used. Note that this field distribution accounts for the magnetic field generated by the strands as a part of the problem; thus, the inclusion of the H_i losses is not required. This logic follows the remark made above, where H_e parameter should not only define the field generated by the rest of the conductors but also the conductor under analysis itself.

Then, it follows that (15) can be used to evaluate the losses in the strands, but the complex definition for $\eta_{(x)}$ and $m_{(x)}$ along the variable geometry in the x-direction makes this complicated. To circumvent this problem, the magnetic field related physical definition of layer presented in [35] can be used, where a layer

is defined as follows:

$$m = \frac{H_{(x=w_c)} - H_{(x=0)}}{H_{(x=w_c)}} \tag{29}$$

where $H_{(x=0)}$ and $H_{(x=w_c)}$ are the magnetic fields to the left and right of the conductor. In the case of circular conductors, w_c is replaced by the strand diameter d_s.

Assuming that the total current in the Litz wire bundle is n_s A so that the current in each strand is normalized to 1 A, the effective increase in the magnetic field per strand is

$$H_{(x=d_s)} - H_{(x=0)} = \frac{N_b}{h_w} \tag{30}$$

where N_b is the amount of Litz wire bundles stacked vertically per layer, and h_w is the height of the core window. Then, the Litz wire geometry can be simplified so that the nth strand in the x-direction has a 1-D average equivalent magnetic field H_e of

$$H_{e(n)} = \frac{N_b}{h_w}\frac{(2n-1)}{2} \tag{31}$$

for m Litz wire layers, then $n = [1..m \cdot n_s]$. Finally, since the losses of each individual strand using Ferreira's equation for round conductors are

$$F_{R,n} = \frac{\gamma}{2}\left(\frac{\mathrm{ber}\,\gamma\,\mathrm{bei}'\,\gamma - \mathrm{bei}\,\gamma\,\mathrm{ber}'\gamma}{\mathrm{ber}'^2\,\gamma + \mathrm{bei}'^2\,\gamma} - \frac{N_b}{h_w}\frac{(2n-1)^2}{2}\frac{\mathrm{ber}_2\,\gamma\,\mathrm{ber}'\,\gamma + \mathrm{bei}_2\,\gamma\,\mathrm{bei}'\gamma}{\mathrm{ber}^2\,\gamma + \mathrm{bei}^2\,\gamma}\right) \tag{32}$$

the definition for the average high-frequency loss increment in all strands becomes

$$F_R = \frac{\gamma}{2}\left(\frac{\mathrm{ber}\,\gamma\,\mathrm{bei}'\,\gamma - \mathrm{bei}\,\gamma\,\mathrm{ber}'\gamma}{\mathrm{ber}'^2\,\gamma + \mathrm{bei}'^2\,\gamma} - \left(\frac{N_b}{h_w}\right)^2\left[\frac{1}{3}\left(m^2 n_s^2 - 1\right) + \frac{1}{4}\right] \times \frac{\mathrm{ber}_2\,\gamma\,\mathrm{ber}'\,\gamma + \mathrm{bei}_2\,\gamma\,\mathrm{bei}'\gamma}{\mathrm{ber}^2\,\gamma + \mathrm{bei}^2\,\gamma}\right). \tag{33}$$

Expression (32) also allows to approximate the losses per Litz strand ordered in ascending x-direction, which allows for a more in-depth comparison with FEM simulations than (33). Unlike the classical Ferreira's approach (27), the analysis of the field per strand removes the intrinsic field averaging errors, which are more noticeable at low number of layers.

Alternatively, based on FEM simulation results, a modified version of Wojda's approach is also proposed. The methodology is the same, but the key difference is that instead of representing the Litz wire strands in a square grid of $n_s^{0.5}$ by $n_s^{0.5}$ dimensions, the strands are distributed into a rectangular grid of $n_s^{0.5-\epsilon}$ stacks and $n_s^{0.5+\epsilon}$ layers, maintaining the total amount of strands equal ($n_s^{0.5-\epsilon} \cdot n_s^{0.5+\epsilon} = n_s$). The value of ϵ is adjusted from the simulation results, where $\epsilon = 0.05$ has been found to give the best overall results. The proximity loss correction factor has also been modified, instead of 0.95, the value $3/\pi$ is used according to Van den Bossche and Valchev [41]. These modifications result in the expression

$$F_R = \Delta \cdot \left(\frac{\sin h2\Delta + \sin 2\Delta}{\cos h2\Delta - \cos 2\Delta} + \frac{\pi}{4}\frac{2\left(n_s^{1+2\epsilon}\cdot m^2 - 1\right)}{3} \times \frac{\sin h\Delta - \sin\Delta}{\cos h\Delta + \cos\Delta}\right) \tag{34}$$

$$\Delta = \sqrt{\frac{\pi}{4}}\frac{d_s}{\delta}\sqrt{n} \tag{35}$$

$$\eta = n_s^{0.5-\epsilon}\, N\sqrt{\frac{\pi}{4}}\frac{d_s}{h_w}. \tag{36}$$

IV. Comparison With Finite-Element Simulations

To evaluate the accuracy of the different models, the 2-D simulations of Litz wires forming transformer winding structures are used. The simulations are carried out using the finite-element method magnetics software [43].

To model the current distribution between Litz wire strands, an equal current is defined in all strands, simulating an ideal strand transposition [44]. According to the authors in [37], [45], and [46], in wires with hundreds of strands, the deviation from homogeneity on strand level has only a very minor influence of bundle-level effects.

The assumption of equally distributed current in the strands also aids in the simulation of Litz wires with high numbers of strands since, at a macroscopic level, the Litz wire can be replaced as a solid wire carrying a homogeneous current density. Assuming a normalized current of 1 A per strands, then

$$J_b = \frac{4n_s}{\pi d_b^2} \tag{37}$$

where J_b is the current density in an equivalent solid wire of equal diameter to the Litz wire bundle d_b. This simplification effectively reduces the computational cost of the FEM simulation, allowing to model Litz wires of high amounts of strands more efficiently.

To model the geometrical strand distribution inside the Litz wire, different assumptions have been used in the literature: radially distributed layers [39], square packing [47], and triangular packing [44]. In reality, the transposition of the strands results in a more disordered arrangement; thus, an alternative distribution is proposed in this article based on the best-known circles in a circle configuration [48]. The angle of each Litz wire is rotated randomly to better depict the unorganized distribution of strands. The differences between internal strand distributions are illustrated in Fig. 4.

The FEM simulations evaluate the impact of four key geometrical parameters in the accuracy of the different 1-D models; number of layers, number of strands, core window fill factor, and Litz wire packing factor. For the base case, a configuration of 3 layers, 200 strands, layer fill factor of $\pi/4$ (closely stacked Litz bundles), and packing factor of 0.65 is considered. The impact of the different parameters is evaluated by deviating from the base case.

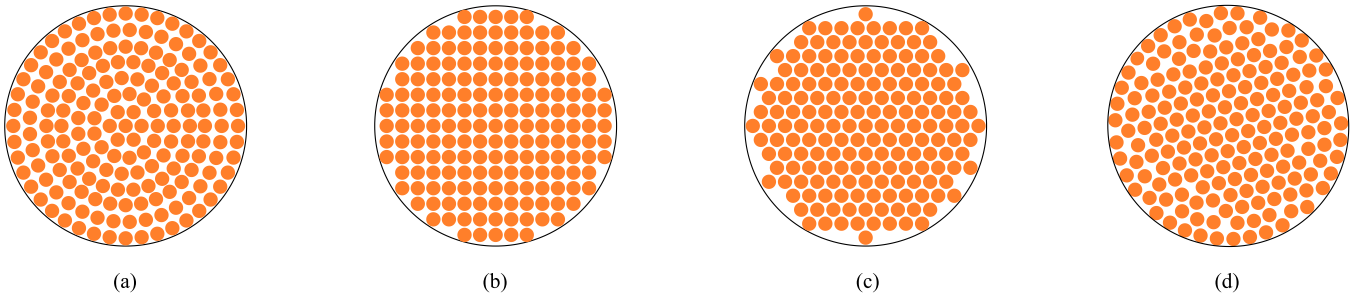

Fig. 4. Different Litz wire strand distribution modeling approaches. (a) Radial layers used in [39]. (b) Square packing used in [47]. (c) Triangular packing used in [44]. (d) Best-known circles in circle with random rotation (this work).

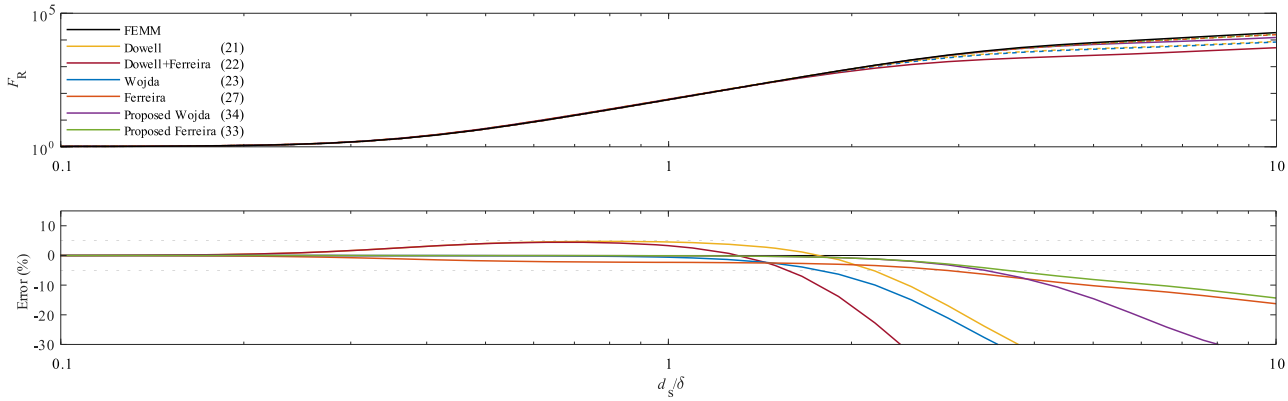

Fig. 5. High-frequency winding loss predictions of the different models in the baseline case ($m = 3$, $n_s = 200$, $\mathrm{PF} = n_s\, d_s^2/\, d_b^2 = 0.65$, and $\eta = \pi/4$).

The results for the baseline case are shown in Fig. 5. Here, the Dowell on Litz (21), Dowell on Litz with Ferreira's modification (22), and Wojda's method (23) are shown for the Dowell-based approaches, as well as Ferreira's Litz wire model (27). The proposed approaches based on Wojda's method (34) and Ferreira's method (33) are also displayed. As can be seen, both (21) and (22) overestimate the losses by a factor of $\pi/3$, as reported by Van den Bossche and Valchev [41], although the modification introduced by Ferreira is noticeable worse at predicting very high frequency losses. Wojda's approach takes this overestimation into account, achieving very accurate predictions, but starts underestimating the losses past $d_s/\delta = 1$. On the contrary, Ferreira's approach for Litz wires is slightly less accurate at low frequencies but retains a higher accuracy at very high frequencies ($d_s/\delta > 1$). Finally, the proposed method based on Wojda's approach can accurately estimate the losses up to higher frequencies than the original Wojda's model, while the proposed approach based on Ferreira's equations achieves similar results to Ferreira's method but with higher accuracies. Based on these results, going forward, only Wojda's model, Ferreira's model for Litz wires, the proposed modified Wojda's approach, and the proposed model based on Ferreira's approach will be analyzed.

When the number of layers is modified, the results change noticeably, as can be seen in Fig. 6. Wojda's model appears to be quite insensitive to the change of layers, while Ferreira's model becomes more accurate as the number of layers is increased since the impact of the error introduced by the averaged H_e diminishes. The opposite is also true for low amounts of layers, where

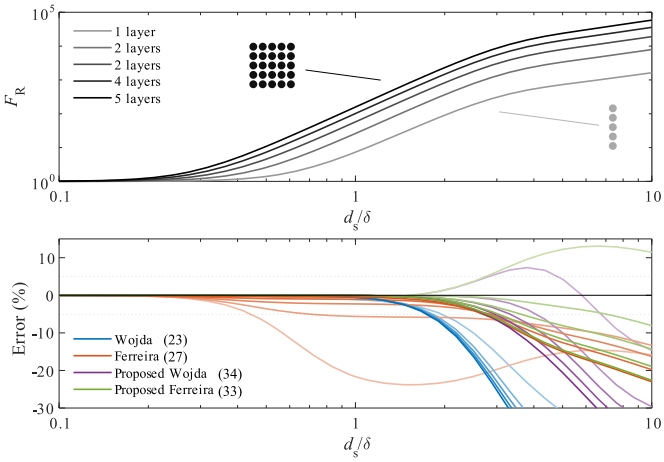

Fig. 6. High-frequency winding loss predictions of the different models for different numbers of layers (m).

Ferreira's model heavily underestimates the proximity losses for the results with one layer. Both the proposed models show similar evolutions with the change in the number of layers; they retain the overall higher accuracies than the preceding models, but overestimate the losses by up to 10%–15% at extremely high frequencies, although these are still better predictions than their counterparts at extreme frequencies.

On the opposite, as shown in Fig. 7, all methods appear to be quite immune to the change in the number of strands,

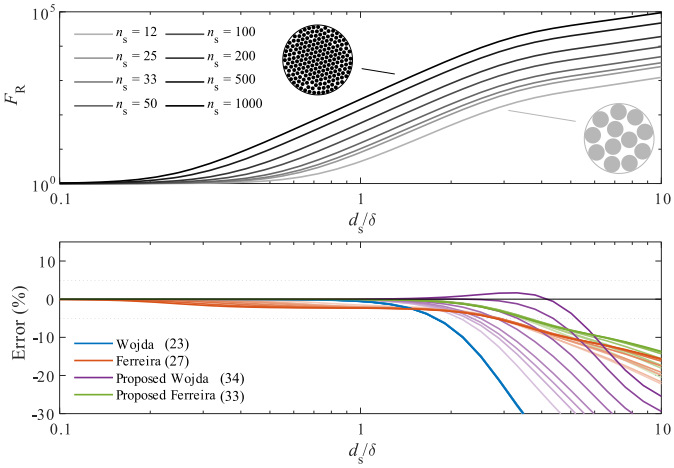

Fig. 7. High-frequency winding loss predictions of the different models for different numbers of Litz strands (n_s).

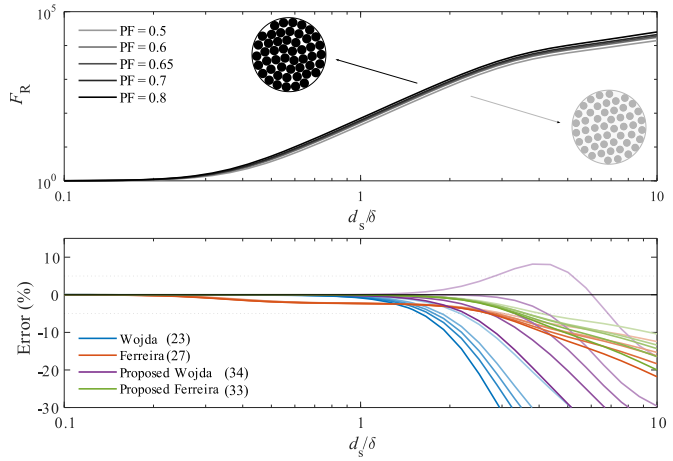

Fig. 8. High-frequency winding loss predictions of the different models for different Litz bundle packing factors ($\mathrm{PF} = n_s d_s^2/d_b^2$).

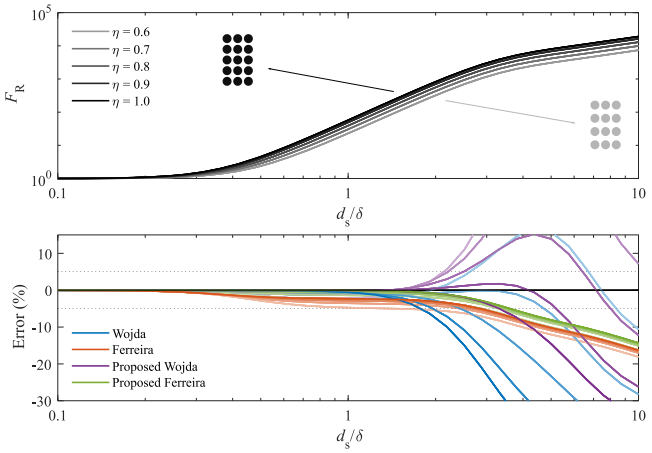

Fig. 9. High-frequency winding loss predictions of the different models for different porosity factors (η).

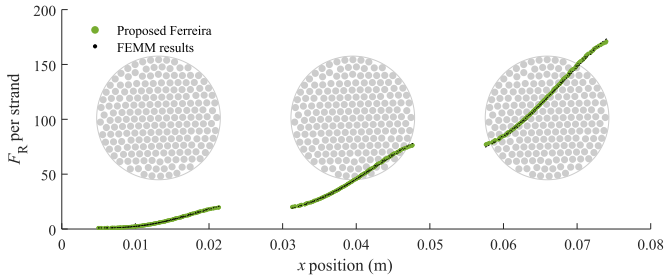

Fig. 10. High-frequency winding loss per strand, simulation results, and prediction using the proposed Ferreira's approach per strand (32).

with very similar results to the baseline case. Wojda's method appears to barely change with the number of strands, showing discrepancies of less than 0.005% between the errors for 12 and 1000 strand simulations, while both Ferreira's model and the proposed Ferreira's model only start changing at very high frequencies ($d_s/\delta > 5$). The only model noticeably affected is the proposed modified Wojda's approach, showing improved accuracies as the number of strands increases. It should be noted that it starts showing a slight overestimation of losses in the transition from high-frequency to very high frequency losses ($d_s/\delta \sim 3$), such as the results with low amounts of layers. FEM simulations with more than 1000 strands are deemed too computationally expensive to evaluate; thus, although the estimations are better than Wojda's approach, the accuracy for very high amounts of strands is uncertain.

The packing factor has a similar impact in all the models, as demonstrated in Fig. 8. The accuracy of Wojda's models is slightly increased for low packing factors, although the model is still unable to give accurate predictions at very high frequencies. Both Ferreira's and the proposed Ferreira's models do not change at all until very high frequencies. The proposed modified Wojda's method shows a similar evolution to the original Wojda's model, but with a much higher sensibility, overestimating the losses in the high-frequency to very high frequency transition at low packing factors.

Finally, the impact of the vertical spacing between wires (porosity factor) is shown in Fig. 9. Both Dowell-based approaches change noticeably with the porosity factor, and the proposed modified Wojda's approach is better at high-porosity factors but shows a higher loss overestimation at very high frequencies. On the contrary, both Ferreira-based approaches appear to be immune to these changes. Although hard to see in Fig. 8, the accuracy of all the models changes similarly up to $d_s/\delta = 1$, all showing around –2.5% error at low-porosity factors compared with the baseline case.

To quantify the results, Table I resumes the obtained maximum and minimum errors of the different methods in the different simulations at $d_s/\delta = 1$. Also, the d_s/δ values where the error surpasses 5% are summarized in Table II. The colors are used to rank the performances of the models.

As mentioned before, the proposed Ferreira's approach-based method has a unique advantage, the capability to estimate the

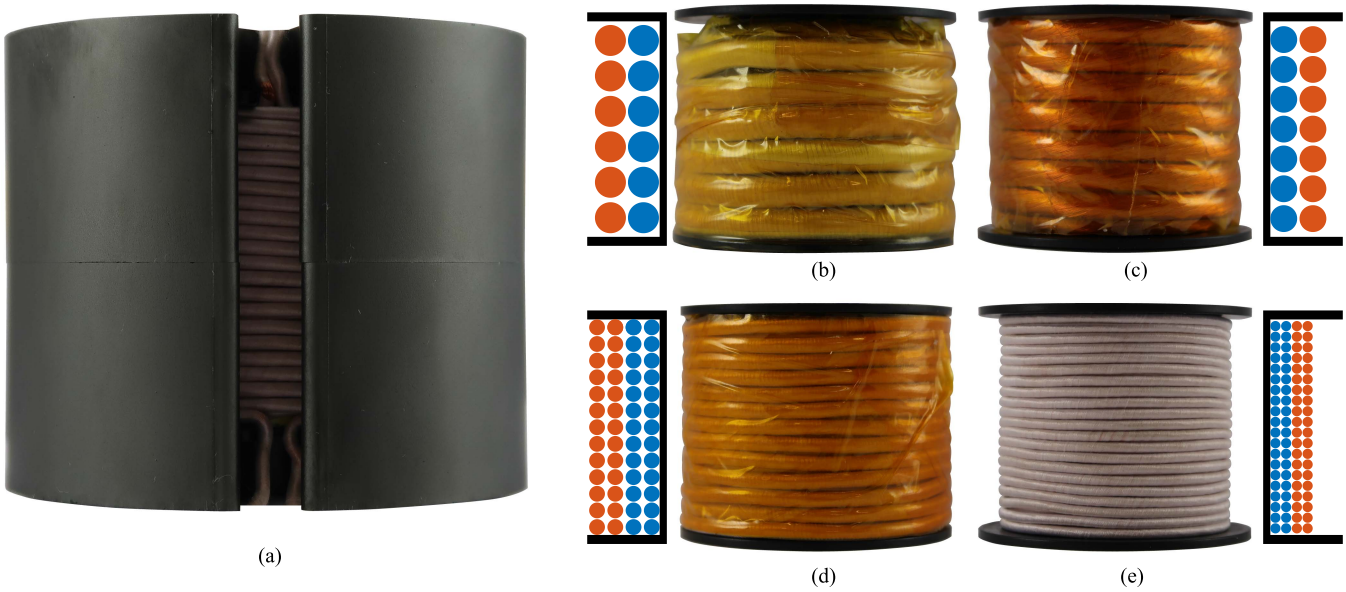

Fig. 11. Photograph of (a) assembled transformer for the resistance measurements and used winding structures. Litz wires used are (b) 400×0.2, (c) 1000×0.1, (d) 400×0.1, and (e) 150×0.1.

TABLE I
ERRORS (%) AT $d_s/\delta = 1$ (LOWER $|E|$ = BETTER)

Simulation	Wojda	Ferreira	Modified Wojda	Proposed Ferreira [REF]
Layers	–0.5063 > E > **–1.1354**	–0.4958 > E > **–21.652**	–0.0159 > E > **–0.6862**	–0.0159 > E > **–0.6315**
Strands	–0.4202 > E > **–0.6147**	–1.5418 > E > –2.3488	+0.0204 > E > **–0.3104**	+0.0848 > E > **–0.1133**
Packing	–0.3090 > E > **–0.8344**	–2.2473 > E > **–2.3545**	+0.0659 > E > **–0.2368**	–0.0262 > E > **–0.1297**
Porosity	–0.5677 > E > **–2.4147**	–2.2994 > E > **–4.7313**	–0.0809 > E > **–2.2359**	–0.0763 > E > **–2.6390**

The bolded value for each scenario represents the worst results for the specific model in the specific scenario.

TABLE II
d_s/δ FOR ERROR > ±5% (HIGHER = BETTER)

Simulation	Wojda	Ferreira	Modified Wojda	Proposed Ferreira
Layers	**1.7310** < $\frac{d_s}{\delta}$ < 1.9463	**0.4414** < $\frac{d_s}{\delta}$ < 2.8633	**2.7335** < $\frac{d_s}{\delta}$ < 4.0525	**2.7474** < $\frac{d_s}{\delta}$ < 6.9914
Strands	**1.7632** < $\frac{d_s}{\delta}$ < 1.7867	**2.7845** < $\frac{d_s}{\delta}$ < 2.9007	**2.1348** < $\frac{d_s}{\delta}$ < 5.2156	**3.4153** < $\frac{d_s}{\delta}$ < 3.6081
Packing	**1.5930** < $\frac{d_s}{\delta}$ < 2.1726	**2.7050** < $\frac{d_s}{\delta}$ < 3.0388	**2.2590** < $\frac{d_s}{\delta}$ < 4.2533	**3.3260** < $\frac{d_s}{\delta}$ < 4.0733
Porosity	**1.7710** < $\frac{d_s}{\delta}$ < 4.7247	**1.4321** < $\frac{d_s}{\delta}$ < 2.8633	**2.1324** < $\frac{d_s}{\delta}$ < 5.1992	**2.8918** < $\frac{d_s}{\delta}$ < 3.6081

The bolded value for each scenario represents the worst results for the specific model in the specific scenario.

losses per strand individually using the alternative expression (32). To show the accuracy of this estimation of losses per strand, the losses per strand of the baseline case at $d_s/\delta = 1$ and the estimated losses per strand from (32) are shown in Fig. 10. Here, the x-axis represents the horizontal position of the individual strands. Although the strands in the border of the Litz wire show a higher error than the rest (the rightmost strand has a prediction error of –1.275%) due to the circular geometry of the Litz wires, more strands are found in the center than in the borders; thus, the impact of this error is reduced.

TABLE III
PARAMETERS OF THE TESTED PROTOTYPES

Strand diameter d_s	Number of strands n_s	Turns per layer N_b	Layers per winding m
0.2 mm	400	6	1
0.1 mm	1000	7	1
0.1 mm	400	13	2
0.1 mm	150	20	2

V. EXPERIMENTAL VALIDATION

To validate the proposed methodology, the experimental setups of short-circuited secondary transformers are prepared and measured using a Bode100. The winding structures and Litz wires used for the four prototypes are shown in Fig. 11. Four prototypes are prepared for the experimental validation according to the parameters from Table III.

To avoid the problems of having inner and outer core windings' sections, common to EE core structures, a pot core that envelopes most of the windings is used. This ensures that the prototypes simulate the hypothesis used to generate the different 1-D models. The windings are excited using a 0.5-V sinusoidal signal. The impedance of the windings structure (primary connected to the Bode100, secondary short circuited) is measured using the configuration from Fig. 12 and the real component used to extract the high frequency resistance.

The obtained results are shown in Fig. 13. Since all the models analyzed achieve similar accuracies at low and mid frequencies, the experimental results focus on the high and very high frequency behaviors ($1 < \Delta < 10$). Prototypes 3 (400×0.1) and 4 (150×0.1) [see Fig. 11(d) and (e)] are made from multiple layers, resulting in high parasitic capacitances; thus, very high frequency range cannot be evaluated correctly. For prototypes 1 (400×0.2) and 2 (1000×0.1) [see Fig. 11(b) and (c)], the

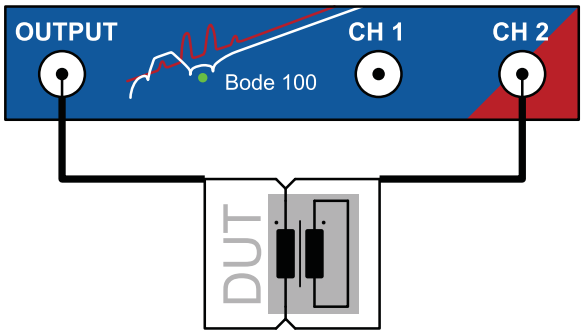

Fig. 12. Experimental setup using the Bode100 shunt-thru measurement.

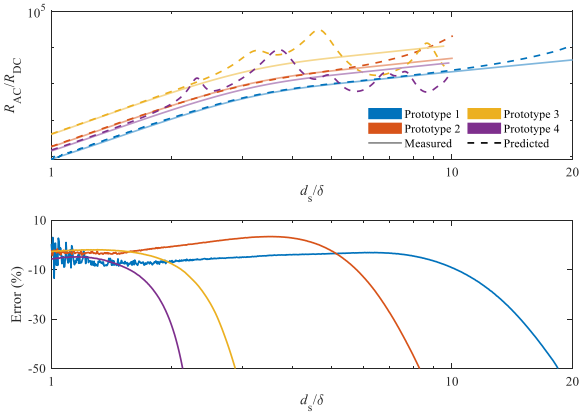

Fig. 13. Experimental measurements and predictions using the proposed Ferreira's approach-based model (32).

parasitic capacitances are much lower; thus, the transition from high to very high frequency can be seen clearly.

VI. Conclusion

In this work, an in-depth analysis of 1-D models for the evaluation of high-frequency winding losses is presented. First, a review of the existing approaches for individual wires is presented, demonstrating the basis of the different approaches based on Dowell's and Ferreira's approach. This is followed by an analysis of the existing approaches to model Litz wire losses with 1-D models.

Next, an alternative approach based on Ferreira's approach to model solid wire losses is presented. Instead of evaluating an average external field to all strands, the evolution of the external field per strand is modeled and used in the calculation of the losses, taking the form (32). This expression allows to evaluate the losses of each strand separately but can also be rewritten to (33) to obtain an average solution analog to the rest of the models presented. Alternatively, a small modification of Wojda's model is also presented, slightly improving the obtained results.

Comparing against FEM simulation, the different models are evaluated and their sensibility to changes in the number of layers, number of strands, Litz packing factor, and fill factor is presented. The results show that how all models accurately estimate the low-frequency losses, except Ferreira's approach in certain conditions. For high to very high frequency ranges, only Ferreira's approach and the proposed model based on Ferreira's approach are capable to attain the accurate results. The proposed modification of Wojda's model is on average more accurate than the original model but is more sensible to all the analyzed variables and can overestimate the losses in extreme cases. Overall, the proposed model based on Ferreira's approach is capable to accurately model the loses in a much wider frequency range. The capabilities of the proposed model to estimate the high-frequency losses per strand are also demonstrated.

Finally, four experimental prototypes using pot cores to achieve magnetic fields of only inner core sections are analyzed. It is shown that the proposed model correctly models the medium- to high-frequency ranges, but the parasitic capacitances of the multilayer prototypes do not allow to evaluate the losses at very high frequencies. On the contrary, the high to very high frequency transition is visible in the single-layer prototypes, demonstrating the capabilities of the proposed model.

References

[1] J. W. Kolar et al., "PWM converter power density barriers," in *Proc. Power Convers. Conf. - Nagoya*, Nagoya, Japan, 2007, pp. P-9–P-29, doi: 10.1109/PCCON.2007.372914.

[2] J. W. Kolar, J. Biela, and J. Minibock, "Exploring the Pareto front of multi-objective single-phase PFC rectifier design optimization - 99.2% efficiency vs. 7kW/din3 power density," in *Proc. IEEE 6th Int. Power Electron. Motion Control Conf.*, Wuhan, China, 2009, pp. 1–21, doi: 10.1109/IPEMC.2009.5289336.

[3] J. W. Kolar, D. Bortis, and D. Neumayr, "The ideal switch is not enough," in *Proc. 28th Int. Symp. Power Semicond. Devices ICs*, Prague, Czech Republic, 2016, pp. 15–22, doi: 10.1109/ISPSD.2016.7520767.

[4] J. Mühlethaler, J. W. Kolar, and A. Ecklebe, "Loss modeling of inductive components employed in power electronic systems," in *Proc. 8th Int. Conf. Power Electron. - ECCE Asia*, Jeju, South Korea, 2011, pp. 945–952, doi: 10.1109/ICPE.2011.5944652.

[5] M. Kasper and G. Deboy, "GaN HEMTs enabling ultra-compact and highly efficient 3kW 12V server power supplies," in *Proc. IEEE Int. Power Electron. Appl. Conf. Expo.*, Shenzhen, China, 2018, pp. 1–6, doi: 10.1109/PEAC.2018.8590433.

[6] M. J. Kasper, L. Peluso, G. Deboy, G. Knabben, T. Guillod, and J. W. Kolar, "Ultra-high power density server supplies employing GaN power semiconductors and PCB-integrated magnetics," in *Proc. 11th Int. Conf. Integr. Power Electron. Syst.*, Berlin, Germany, 2020, pp. 1–8.

[7] W.-J. Gu and R. Liu, "A study of volume and weight vs. frequency for high-frequency transformers," in *Proc. IEEE Power Electron. Specialist Conf.*, Seattle, WA, USA, 1993, pp. 1123–1129, doi: 10.1109/PESC.1993.472059.

[8] M. Mogorovic and D. Dujic, "100 kW, 10 kHz medium-frequency transformer design optimization and experimental verification," *IEEE Trans. Power Electron.*, vol. 34, no. 2, pp. 1696–1708, Feb. 2019, doi: 10.1109/TPEL.2018.2835564.

[9] M. Mogorovic and D. Dujic, "Sensitivity analysis of medium-frequency transformer designs for solid-state transformers," *IEEE Trans. Power Electron.*, vol. 34, no. 9, pp. 8356–8367, Sep. 2019, doi: 10.1109/TPEL.2018.2883390.

[10] M. Leibl, G. Ortiz, and J. W. Kolar, "Design and experimental analysis of a medium-frequency transformer for solid-state transformer applications," *IEEE J. Emerg. Sel. Topics Power Electron.*, vol. 5, no. 1, pp. 110–123, Mar. 2017, doi: 10.1109/JESTPE.2016.2623679.

[11] F. C. Lee, Q. Li, Z. Liu, Y. Yang, C. Fei, and M. Mu, "Application of GaN devices for 1 kW server power supply with integrated magnetics," *CPSS Trans. Power Electron. Appl.*, vol. 1, no. 1, pp. 3–12, Dec. 2016, doi: 10.24295/CPSSTPEA.2016.00002.

[12] G. Li and X. Wu, "High power density 48–12 V DCX with 3-D PCB winding transformer," *IEEE Trans. Power Electron.*, vol. 35, no. 2, pp. 1189–1193, Feb. 2020, doi: 10.1109/TPEL.2019.2933595.

[13] M. H. Ahmed, C. Fei, F. C. Lee, and Q. Li, "48-V voltage regulator module with PCB winding matrix transformer for future data centers," *IEEE Trans. Ind. Electron.*, vol. 64, no. 12, pp. 9302–9310, Dec. 2017, doi: 10.1109/TIE.2017.2711519.

[14] R. Yu, T. Chen, P. Liu, and A. Q. Huang, "A 3-D winding structure for planar transformers and its applications to LLC resonant converters," *IEEE J. Emerg. Sel. Topics Power Electron.*, vol. 9, no. 5, pp. 6232–6247, Oct. 2021, doi: 10.1109/JESTPE.2021.3052712.

[15] A. Furlan and M. L. Heldwein, "Considering 2D magnetic fields and air gap geometry in the estimation of AC losses in round wire windings," in *Proc. Int. Exhib. Conf. Power Electron., Intell. Motion, Renewable Energy Energy Manage.*, Nuremberg, Germany, 2023, pp. 1–8, doi: 10.30420/566091060.

[16] F. A. Holguín, R. Prieto, R. Asensi, and J. A. Cobos, "Power losses calculations in windings of gapped magnetic components: The extended 2-D method," in *Proc. IEEE Appl. Power Electron. Conf. Expo.*, Charlotte, NC, USA, 2015, pp. 128–132, doi: 10.1109/APEC.2015.7104342.

[17] F. A. Holguin, R. Prieto, R. Asensi, and J. A. Cobos, "Power losses calculations in windings of gapped magnetic components: The i2D method applied to flyback transformers," in *Proc. IEEE Energy Convers. Congr. Expo.*, Montreal, QC, Canada, 2015, pp. 5675–5681, doi: 10.1109/ECCE.2015.7310457.

[18] W. A. Roshen, "High-frequency fringing fields loss in thick rectangular and round wire windings," *IEEE Trans. Magn.*, vol. 44, no. 10, pp. 2396–2401, Oct. 2008, doi: 10.1109/TMAG.2008.2002302.

[19] W. Water and J. Lu, "Improved high-frequency planar transformer for line level control (LLC) resonant converters," *IEEE Magn. Lett.*, vol. 4, Nov. 2013, Art. no. 6500204, doi: 10.1109/LMAG.2013.2284767.

[20] R. Pittini, Z. Zhang, and M. A. E. Andersen, "High current planar transformer for very high efficiency isolated boost dc-dc converters," in *Proc. Int. Power Electron. Conf.*, Hiroshima, Japan, 2014, pp. 3905–3912, doi: 10.1109/IPEC.2014.6870060.

[21] C. Lian and D. Zhang, "Field-circuit analysis of planar transformer at medium frequency for converter application," in *Proc. IEEE 2nd Annu. Southern Power Electron. Conf.*, Auckland, New Zealand, 2016, pp. 1–5, doi: 10.1109/SPEC.2016.7846127.

[22] R. Zhang, D. Zhang, and R. Dutta, "Study on PCB based Litz wire applications for air-core inductor and planar transformer," in *Proc. 9th Int. Conf. Power Energy Syst.*, Perth, WA, Australia, 2019, pp. 1–6, doi: 10.1109/ICPES47639.2019.9105549.

[23] S. Wang, M. A. de Rooij, W. G. Odendaal, J. D. van Wyk, and D. Boroyevich, "Reduction of high-frequency conduction losses using a planar Litz structure," *IEEE Trans. Power Electron.*, vol. 20, no. 2, pp. 261–267, Mar. 2005, doi: 10.1109/TPEL.2004.843022.

[24] C. R. Sullivan, "Cost-constrained selection of strand diameter and number in a Litz-wire transformer winding," *IEEE Trans. Power Electron.*, vol. 16, no. 2, pp. 281–288, Mar. 2001, doi: 10.1109/63.911153.

[25] C. R. Sullivan and R. Y. Zhang, "Simplified design method for Litz wire," in *Proc. IEEE Appl. Power Electron. Conf. Expo.*, Fort Worth, TX, USA, 2014, pp. 2667–2674, doi: 10.1109/APEC.2014.6803681.

[26] P. L. Dowell, "Effects of eddy currents in transformer windings," *Proc. IEE*, vol. 113, no. 8, pp. 1387–1394, Aug. 1966.

[27] J. A. Ferreira, "Appropriate modelling of conductive losses in the design of magnetic components," in *Proc. 21st Annu. IEEE Conf. Power Electron. Specialists*, San Antonio, TX, USA, 1990, pp. 780–785, doi: 10.1109/PESC.1990.131268.

[28] J. A. Ferreira, "Improved analytical modeling of conductive losses in magnetic components," *IEEE Trans. Power Electron.*, vol. 9, no. 1, pp. 127–131, Jan. 1994, doi: 10.1109/63.285503.

[29] X. Nan and C. R. Sullivan, "Simplified high-accuracy calculation of eddy-current loss in round-wire windings," in *Proc. IEEE 35th Annu. Power Electron. Specialists Conf.*, Aachen, Germany, 2004, vol. 2, pp. 873–879, doi: 10.1109/PESC.2004.1355533.

[30] X. Nan and C. R. Sullivan, "An improved calculation of proximity-effect loss in high-frequency windings of round conductors," in *Proc. IEEE 34th Annu. Conf. Power Electron. Specialist*, Acapulco, Mexico, 2003, vol. 2, pp. 853–860, doi: 10.1109/PESC.2003.1218168.

[31] R. P. Wojda and M. K. Kazimierczuk, "Winding resistance of Litz-wire and multi-strand inductors," *IET Power Electron.*, vol. 5, no. 2, pp. 257–268, Feb. 2012, doi: 10.1049/iet-pel.2010.0359.

[32] M. Kaymak, Z. Shen, and R. W. De Doncker, "Comparison of analytical methods for calculating the AC resistance and leakage inductance of medium-frequency transformers," in *Proc. IEEE 17th Workshop Control Model. Power Electron.*, Trondheim, Norway, 2016, pp. 1–8, doi: 10.1109/COMPEL.2016.7556740.

[33] E. Bennett and S. C. Larson, "Effective resistance to alternating currents of multilayer windings," *Elect. Eng.*, vol. 59, no. 12, pp. 1010–1016, Dec. 1940, doi: 10.1109/EE.1940.6435274.

[34] S. Butterworth and F. E. Smith, "III. Eddy-current losses in cylindrical conductors, with special applications to the alternating current resistances of short coils," *Philos. Trans. Roy. Soc. A, Math., Physical, Eng. Sci.*, vol. 222, pp. 57–100, 1922.

[35] M. P. Perry, "Multiple layer series connected winding design for minimum losses," *IEEE Trans. Power App. Syst.*, vol. PAS-98, no. 1, pp. 116–123, Jan. 1979, doi: 10.1109/TPAS.1979.319520.

[36] F. Robert, P. Mathys, and J.-P. Schauwers, "The layer copper factor, although widely used and useful, has no theoretical base [SMPS transformers]," in *Proc. IEEE 31st Annu. Power Electron. Specialists Conf.*, Galway, Ireland, 2000, vol. 3, pp. 1633–1638, doi: 10.1109/PESC.2000.880549.

[37] C. R. Sullivan, "Optimal choice for number of strands in a Litz-wire transformer winding," *IEEE Trans. Power Electron.*, vol. 14, no. 2, pp. 283–291, Mar. 1999, doi: 10.1109/63.750181.

[38] J. A. Ferreira and J. D van Wyk, "A new method for the more accurate determination of conductor losses in power electronic converter magnetic components," in *Proc. 3rd Int. Conf. Power Electron. Variable-Speed Drives*, London, U.K., 1988, pp. 184–187.

[39] M. Bartoli, N. Noferi, A. Reatti, and M. K. Kazimierczuk, "Modelling winding losses in high-frequency power inductors," *J. Circuits, Syst. Comput.*, vol. 5, no. 4, pp. 607–626, 1995, doi: 10.1142/S0218126695000370.

[40] A. Reatti and M. K. Kazimierczuk, "Comparison of various methods for calculating the AC resistance of inductors," *IEEE Trans. Magn.*, vol. 38, no. 3, pp. 1512–1518, May 2002, doi: 10.1109/20.999124.

[41] A. Van den Bossche and V. C. Valchev, *Inductors and Transformers for Power Electronics*. Boca Raton, FL, USA: Taylor & Francis, 2005.

[42] J. A. Ferreira, "Analytical computation of AC resistance of round and rectangular Litz wire windings," *IEE Proc. B (Electr. Power Appl.)*, vol. 139, no. 1, pp. 21–25, 1992, doi: 10.1049/ip-b.1992.0003.

[43] D. C. Meeker, "Finite element method magnetics," Version 4.2 (28 Feb 2018 Build), 2018. [Online]. Available: https://www.femm.info

[44] S. Cruciani, T. Campi, F. Maradei, and M. Feliziani, "Numerical modeling of Litz wires based on discrete transpositions of strands and 2-D finite element analysis," *IEEE Trans. Power Electron.*, vol. 38, no. 5, pp. 6710–6719, May 2023, doi: 10.1109/TPEL.2023.3240338.

[45] A. Roßkopf, E. Bär, C. Joffe, and C. Bonse, "Calculation of power losses in Litz wire systems by coupling FEM and PEEC method," *IEEE Trans. Power Electron.*, vol. 31, no. 9, pp. 6442–6449, Sep. 2016, doi: 10.1109/TPEL.2015.2499793.

[46] M. Albach, "Two-dimensional calculation of winding losses in transformers," in *Proc. IEEE 31st Annu. Power Electron. Specialists Conf.*, Galway, Ireland, 2000, vol. 3, pp. 1639–1644, doi: 10.1109/PESC.2000.880550.

[47] V. Väisänen, J. Hiltunen, J. Nerg, and P. Silventoinen, "AC resistance calculation methods and practical design considerations when using Litz wire," in *Proc. 39th Annu. Conf. IEEE Ind. Electron. Soc.*, Vienna, Austria, 2013, pp. 368–375, doi: 10.1109/IECON.2013.6699164.

[48] E. Specht, "The best known packings of equal circles in a circle (complete up to N = 2600)." 2000. [Online]. Available: http://hydra.nat.uni-magdeburg.de/packing/cci/cci.html